J. Phys. Chem. A **1998,** *102,* 9869−9875

Ab Initio Study of the Mechanism for the Reaction of CF_2 Radicals with OH

Ruifeng Liu

Department of Chemistry, East Tennessee State University, Johnson City, Tennessee 37614-0695

Joseph S. Francisco*

Department of Chemistry and Department of Earth and Atmospheric Sciences, Purdue University,
West Lafayette, Indiana 47907-1393

Received: April 9, 1998; In Final Form: September 17, 1998

The reaction of difluorocarbene (CF_2) radicals with OH is studied by *ab initio* molecular orbital theory. The potential energy surface of the reaction system is explored with density functional theory (B3LYP) and second-order Møller−Plesset perturbation theory (MP2). The quadratic configuration interaction [QCISD(T)] method is used to compute the energetics. The mechanism of the reaction is proposed for the first time. It is found that the major products of the reaction are CF_2O and H atoms. The products can be produced through the CF_2OH or CHF_2O intermediates involved in the reaction. The suggestion of CF_2O as a product of the CF_2 + OH reaction is consistent with experiments.

I. Introduction

Halons, which are bromine-containing hydrocarbons, have found wide use as fire extinguisher materials.[1−3] Halon 1301 (CF_3Br) is used primarily in automatic fire-extinguishing systems, while Halon 1211 (CF_2ClBr) is used in portable fire extinguishers. Because of concern over the depletion of ozone in the atmosphere by halons such as Halon 1301 and Halon 1211, the use of these materials has been targeted to be banned by the turn of the century. As a result, there has been a search for suitable alternatives as drop-in replacements. To be an ideal replacement, the new materials must exhibit high flame-suppression efficiency. The need for environmentally friendly alternatives that have flame-inhibition efficiencies equal to or better than Halon 1301 and Halon 1211 is critical to narrowing the choice of substitutes. Understanding how new materials suppress flames involves the need to understand the underlying chemical mechanism. Several studies have suggested that radical species such as CF_3, CF_2, and FCO are primarily responsible for flame suppression.[4−7] However, few studies have reported direct detection of these radicals in flames. Usually the combustion product, CF_2O, is observed from *in situ* spectroscopic studies of the flame.[8] A recent study of alternative HFC-134a and HCFC-22 in H_2 and CH_4 flames using laser-induced fluorescence has revealed the first direct spectroscopic detection of CF_2 radicals *in situ*.[9] In H_2 and CH_4 flames, one of the major radical species is OH radicals. A question we have asked is what the products of the reaction of CF_2 with OH radicals are and what the mechanism by which the products are produced is. Biordi et al.[10] have suggested that CF_2 produced in flames is a principal result of the reaction of CF_3 radicals with hydrogen atoms via the following:

$$CF_3 + H \rightarrow HF + CF_2 \qquad (1)$$

Biordi et al.[10] have suggested that a major decay channel for CF_2 radicals is reaction with major flame radicals such as the OH radical. However, they could not identify the products of the CF_2 + OH reaction. No experimental studies to date have examined this fundamental chemical reaction. To understand the details of the CF_2 + OH reaction, *ab initio* calculations have been performed to determine relative thermodynamic and activation energetics for pathways which result in the decay of CF_2 radicals by reaction with OH radicals.

II. Computational Methods

All calculations were performed using the GAUSSIAN 94 program.[11] Geometry optimizations were carried out for all structures using Schlegel's method[12] to better than 0.001 Å for bond lengths and 0.01° for angles, with a self-consistent field convergence of at least 10^{-9} on the density matrix. The residual rms force is less than 10^{-4} a.u. Initial searches for the transition states were performed at the B3LYP/6-31G(d,p) level of theory.[13,14] Once the transition states were found, vibrational frequencies were calculated analytically to verify if the transition state was a first-order saddle point. To check whether the saddle point led to the correct reactants and products, an intrinsic reaction coordinate (IRC) calculation was performed. The geometries and second derivatives from the B3LYP/6-31G(d,p) searches were then used in optimizations with second-order Møller−Plesset (MP2) level[15,16] of theory with the enlarged 6-311G(d,p) basis set. The basis set was further enlarged by supplementing it with additional sets of polarization functions on all the heavy atoms and the hydrogen as well as the addition of diffuse functions on all heavy atoms and hydrogen. Single point energies are calculated for optimized geometries obtained at the UMP2/6-311++G(2d,2p) level of theory with the quadratic configuration interaction method with single and double excitations (QCISD) and with perturbative corrections for triple excitations [QCISD(T)].[17,18] We have examined the spin contamination before and after annihilation for the radical species and transition states involved in the CF_2 + OH reaction. Before annihilation $\langle s^2 \rangle$ ranges from 0.809 to 0.752, and after annihilation $\langle s^2 \rangle$ is 0.750. This suggests that the wave function is not strongly contaminated by states of higher multiplicity.

---

* Author to whom correspondence should be addressed.

10.1021/jp981804s CCC: $15.00

Moreover, this suggests that a single determinant reference wave function for these systems is suitable for the various levels of theory used in the optimizations.

To help future spectroscopic identification of the intermediates of the $CF_2 + OH$ reaction, we calculated excitation energies of the intermediates to the low-lying excited states by state-average complete active space SCF (sa-CASSCF),[18,19] followed by internally contracted multireference configuration interaction with single and double excitations (MRCISD)[20] in order to include dynamical correlation effects. The use of sa-CASSCF is to avoid bias toward any state. Both the ground and excited states were simultaneously optimized in the sa-CASSCF calculations with equal weight. The natural orbitals obtained from diagonalizing sa-CASSCF density matrices were used in subsequent MRCISD calculations. For the CF_2OH radical, because of the lack of molecular symmetry a small CASSCF active space of three electrons in three active orbitals was used in order for the subsequent MRCISD calculations to be manageable. With such a small active space, the results of CASSCF are not expected to be accurate. For CF_2HO radical, because of CS molecular symmetry the MRCISD calculation is less expensive and we can afford to use a larger CASSCF reference wave function. To get the best estimate of excitation energies, the CASSCF active space is nine electrons in six active orbitals. The CASSCF and MRCISD calculations were performed with MOLPRO.[21]

III. Results and Discussion

Table 1 contains optimized geometries for all species involved in the $CF_2 + OH$ reaction. The vertical excited-state energies for the intermediates involved in the reactions are given in Tables 2 and 3. Vibrational frequencies and zero-point energies are presented in Table 4, and the total energies are given in Table 5. Relative energies of the reactions involved are listed in Table 6 and Table 7. The experimental heats of formation for reactant and product species from the literature are given in Table 8.

A. Intermediates of the $CF_2 + OH$ Reaction. There are two intermediates that could be involved in the $CF_2 + OH$ reaction: (1) a CF_2OH radical and (2) a CHF_2O radical. The CF_2OH radical results from the addition of CF_2 to OH radicals. The CHF_2O radical results from the isomerization of CF_2OH radicals. We have optimized the structures for both intermediates. For the CF_2OH radical, the structure is nonplanar (see Figure 1 and Table 1). The OH group lies out of the FCO plane. The OCFF′ angle for CF_2OH is 126.8°. In CF_2O, the CO bond is 1.177 Å. In CF_2OH, the same bond is 1.345 Å, which is quite close to a CO single bond. This CO single-bond length in CF_2OH is similar to the CO bond in CF_3OH, which has been estimated to range between 1.33 and 1.350 Å. In CF_2OH, electron delocalization also appears to occur across the CF bonds. For CF_2OH, the CF and CF′ bonds are predicted to be 1.323 and 1.346 Å, respectively. These bonds are larger than the CF bond in CF_2, which is predicted to be 1.303 Å at the MP2/6-311++G(2d,2p) level of theory. They are also larger than the CF bond in CF_2O of 1.321 Å at the same level of theory. An examination of the spin-density matrix reveals a significant delocalization of electron spin across the CF bond, which causes weakening of the CF bond and hence produces a larger CF bond in CF_2OH than in CF_2O.

Because the CF_2OH radical plays an important role in the chemical mechanism for the $CF_2 + OH$ reaction, as we shall see later, we have calculated vertical excitations for the first excited state of the CF_2OH radical. This is done to aid in the

TABLE 1: Optimized Bond Lengths (Å) and Angles (degrees) for Reactants, Intermediates, Products, and Transition State of the $CF_2 + OH$ Reaction

species	coordinate	B3LYP/ 6-31G(d,p)	UMP2/ 6-311++G(2d,2p)
Reactants and Products			
HF	HF	0.925	0.918
CF	CF	1.287	1.277
OH	OH	0.980	0.966
HOF	HO	0.974	0.966
	FO	1.434	1.436
	HOF	97.9	97.8
FCO	CF	1.336	1.335
	CO	1.178	1.170
	FCO	127.3	128.1
CF_2	CF	1.313	1.303
	FCF	104.1	104.9
CF_2O	CF	1.322	1.321
	CO	1.180	1.177
	FCO	126.1	126.2
CHFO	CH	1.097	1.088
	CF	1.346	1.354
	CO	1.186	1.184
	HCO	127.5	128.1
	FCO	123.1	122.8
Intermediates			
CF_2OH	CO	1.351	1.345
	CF	1.330	1.323
	CF′	1.353	1.346
	OH	0.968	0.962
	HOC	108.2	108.2
	OCF	110.0	110.1
	OCF′	113.6	114.1
	FCF	110.5	110.4
	HOCF	−175.5	−178.2
	OCFF′	126.3	126.8
CHF_2O	CO	1.332	1.344
	CH	1.114	1.092
	CF	1.358	1.355
	HCO	103.1	105.5
	FCO	113.8	112.2
	FCF	106.9	106.6
	OCFF	126.5	123.2
	OCHF	121.5	121.3
Transition State			
$[CF_2OH \rightarrow HF + FCO]^{\ddagger}$	CO	1.262	1.257
	HO	1.225	1.207
	HF	1.205	1.227
	CF′	1.725	1.730
	CF	1.314	1.330
	HOC	80.1	80.5
	F′CO	91.1	91.3
	OCF	122.2	122.8
	HOCF′	3.7	4.2
	HOCF	117.7	119.3
$[CF_2OH \rightarrow CHF_2O]^{\ddagger}$	CO	1.333	1.312
	HO	1.218	1.235
	CH	1.293	1.260
	CF	1.337	1.331
	HCO	55.2	57.4
	FCF	109.2	108.8
	FCO	118.1	119.2
	FCOH	112.5	111.3
$[CF_2OH \rightarrow CF_2O + H]^{\ddagger}$	CO	1.216	1.202
	CF	1.323	1.313
	OH	1.445	1.322
	HOC	118.9	118.8
	OCF	124.5	124.5
	FCF	109.4	109.3
	HOCF	81.8	81.6
$[CF_2HO \rightarrow CF_2O + H]^{\ddagger}$	CO	1.201	1.192
	CH	1.679	1.450
	CF	1.335	1.339
	OCF	124.7	124.5
	OCH	94.2	92.6
	OCFH	49.7	125.6
$[CF_2HO \rightarrow CHFO + F]^{\ddagger}$	CO	1.208	1.210
	CH	1.094	1.085
	CF	1.330	1.323
	CF′	2.097	1.785
	OCF	122.1	121.7
	OCF′	78.7	84.1
	OCH	126.9	126.0
	OCFF′	86.2	91.1
	OCFH	−173.5	−165.5
$[CF_2HO \rightarrow HF + FCO]^{\ddagger}$	CO	1.199	1.173
	CF	1.325	1.318
	CH	1.137	1.287
	CF′	1.821	1.637
	HF′	1.609	1.373
	FCO	124.7	128.7
	F′CO	117.9	120.5
	FCH	112.1	107.3
	HCF′	60.8	54.4
	OCFH	162.6	157.9
	OCF′H	−111.7	−107.3

TABLE 2: Calculated Vertical Excitation Energies for the CF_2OH Radical

	total energy (hartrees)		
	ground state	1st excited state	relative energy (kcal mol^{-1}) ΔE
SA-CASSCF (3e,3o)	−312.173410	−311.954770	137.2
MRCISD	−312.821191	−312.607590	134.0
MRCISD + Davidson corr.	−312.910262	−312.701618	130.9
most important configurations in the active orbital	$16a^2 17a^1 18a^0$	$16a^2 17a^0 18a^1$	

TABLE 3: Calculated Vertical Excitation Energies for the CHF_2O Radical

	total energies (hartrees)				relative energy		
	X^2A'	$1^2A'$	$1^2A''$	$2^2A''$	$1^2A'$	$1^2A''$	$2^2A''$
SA-CASSCF (9e,6o)	−312.178866	−312.168767	−312.023666	-311.850354	6.3	97.4	206.1
MRCISD	−312.813518	−312.670124	−312.800608	-312.548644	90.0	8.1	166.2
MRCISD + Davidson corr.	−312.900705	−312.764092	−312.886772	-312.667996	85.7	8.7	146.0
most important configurations in the active orbitals	$10a'^2 11a' 4a''^2 5a''^2 6a''^2$	$10a' 11a'^2 4a''^2 5a''^2 6a''^2$	$10a'^2 11a'^2 4a''^2 5a''^2 6a''$	$10a'^2 11a'^2 4a''^2 5a'' 6a''^2$			

TABLE 4: Vibrational Frequencies (cm^{-1}) and Zero-Point Energies (kcal mol^{-1}) Calculated at the B3YLP/6-31G(d,p) Level of Theory

molecules	vibrational frequencies	zero-point energy (ZPE)
	Reactants and Products	
HF	4089	5.8
CF	1316	1.9
OH	3694	5.3
HOF	3734, 1396, 999	8.8
FCO	1926, 1074, 627	5.2
CF_2	1251, 1143, 658	4.4
CF_2O	1996, 1283, 877, 674, 613, 571	8.9
CHFO	3102, 1914, 1399, 1115, 1043, 666	13.2
	Intermediates	
CF_2OH	3826, 1383, 1276, 1102, 1054, 686, 497, 495, 268	15.1
CHF_2O	2885, 1335, 1286, 1159, 1119, 953, 611, 496, 472	14.8
	Transition States	
$CF_2OH \rightarrow [FCO + HF]^‡$	2057, 1583, 1186, 931, 766, 717, 595, 250, 1652i	11.6
$CF_2OH \rightarrow [CHF_2O]^‡$	2352, 1329, 1231, 1016, 696, 641, 516, 494, 1992i	11.8
$CF_2OH \rightarrow [CF_2O + H]^‡$	1781, 1303, 962, 850, 597, 555, 509, 269, 1371i	9.8
$CHF_2O \rightarrow [CF_2O + H]^‡$	1804, 1233, 970, 793, 622, 607, 518, 477, 1049i	10.0
$CHF_2O \rightarrow [CFHO + F]^‡$	3138, 1752, 1396, 1155, 998, 661, 280, 153, 102i	13.6
$CHF_2O \rightarrow [FCO + HF]^‡$	2647, 1736, 1171, 1126, 772, 562, 540, 277, 460i	12.6

future spectroscopic identification of these important species involved in the chemical mechanism for the $CF_2 + OH$ reaction. The vertical excitations for the CF_2OH intermediate are given in Table 2. Using a state-average CASSCF wave function, the first excited state is located at 137.2 kcal mol^{-1} above the ground state (at 208 nm). Using the CASSCF wave function as the reference wave function for the multireference configuration interaction method with single and double excitations, hence a MRCISD calculation, the vertical transition for the first excited state shifts by 3.2 kcal mol^{-1} lower in energy. When the Davidson correction is applied, an estimation of the first excited-state vertical transition is 130.9 kcal mol^{-1}, which is at 218 nm.

The next intermediate in the $CF_2 + OH$ reaction is the CHF_2O radical, shown in Figure 1b, which results from the isomerization of the CF_2OH intermediates. There has been one other previously reported optimization for the CHF_2O structure in the literature. Francisco and Zhao[22] reported UMP2/6-311G(d,p) optimizations for the CHF_2O radical. With the addition of diffuse functions to all atoms and an extra set of d-polarization functions to all the heavy atoms as well as an extra set of p-polarization functions to the hydrogens with the 6-311G(d,p) basis set, the agreement between the two calculated structures is consistent. For example, the CO bond length in CHF_2O at the /6-311G(d,p) level of theory reported by Francisco and Zhao is 1.342 Å. At the UMP2/6-311++G(2d,2p) level of theory reported in this work, the CO bond length is 1.344 Å. Similarly, the CF bond length with the UMP2/6-311G(d,p) basis set is 1.349 Å, while the UMP2/6-311G(2d,2p) result is 1.346 Å. Like CF_2OH UMP2, we have estimated vertical excitation energies for the CHF_2O radical. These results are reported in Table 3. The unpaired electron in the CHF_2O radical resides mainly on the oxygen atom, and can be in either the p_x or the p_y orbital of oxygen. The ground state of the CHF_2O radical is in the $^2A'$ state in which the electron is in the p_x orbital in-the-plane. The lowest $^2A''$ state results from the electron in the p_y orbital in the out-of-plane. The $1^2A''$ state is 8.7 kcal mol^{-1} above the ground state (X^2A'). This is not too surprising since the p_x and p_y orbitals should be quite close in energy. The $1^2A'$ state is 85.7 kcal mol^{-1} above the ground X^2A' state, suggesting that the vertical transition state should be located near 334 nm. This transition results from the promotion of the unpaired electron from the p_x orbital to the p_z orbital (in the molecular plane). This orbital is an antibonding oxygen orbital. A similar electronic state transition is predicted and observed for the X−A transition for the CF_3O radical.[23−25] The X−A transition in CF_3O involves a promotion of an electron from the out-of-plane

TABLE 5: Total Energies (hartrees) for Species Involved in the CF_2 + OH Reaction

	6-31G(d,p)	6-311++G(2d,2p)			6-311++G(2df,2p)
species	B3LYP	MP2	QCISD	QCISD(T)	QCISD(T)
		Reactants and Products			
H	−0.50027	−0.49981	−0.49981	−0.49981	−0.49981
F	−99.71553	−99.57860	−99.58917	−99.59209	−99.61391
HF	−100.42746	−100.30306	−100.30454	−100.39900	−100.33316
CF	−137.77696	−137.53505	−137.55109	−137.56157	−137.59700
OH	−75.72848	−75.59737	−75.61078	−75.61506	−75.63361
HOF	−175.52767	−175.25646	−175.26247	−175.27783	−175.32327
FCO	−213.09475	−212.73439	−212.73768	−212.75863	−212.81843
CF_2	−237.68975	−237.31307	−237.32221	−237.34111	−237.40590
CF_2O	−313.00795	−312.51237	−312.50938	−312.53684	−312.62637
CHFO	−213.76432	−213.40094	−213.40434	−213.42543	−213.48660
		Intermediates			
CF_2OH	−313.54195	−313.03642	−313.04358	−313.06823	−313.15632
CHF_2O	−313.53044	−313.01204	−313.02931	−313.05250	−313.13965
		Transition States			
$CF_2OH \rightarrow [FCO + HF]^\ddagger$	−313.47614	−312.96493	−312.96564	−312.99533	−313.08151
$CF_2OH \rightarrow [CF_2O + H]^\ddagger$	−313.49156	−312.96790	−312.97947	−313.00704	−313.09697
$CF_2OH \rightarrow [CHF_2O]^\ddagger$	−313.48162	−312.97051	−312.97473	−313.00476	−313.09150
$CHF_2O \rightarrow [CF_2O + H]^\ddagger$	−313.49642	−312.97855	−312.99199	−313.01884	−313.10826
$CHF_2O \rightarrow [CHFO + F]^\ddagger$	−313.48558	−312.95273	−312.97993	−313.00676	−313.09178
$CHF_2O \rightarrow [FCO + HF]^\ddagger$	−313.48716	−312.95589	−312.96254	−312.99318	−313.08007

TABLE 6: Heats of Reaction (kcal mol^{-1}) for CF_2 + OH Reaction Pathways

level of theory	CF_2 + OH → FCO + HF	CF_2 + OH → CF_2O + H	CF_2 + OH → CF + FOH	CF_2 + OH → CF_2OH	CF_2OH → CHF_2O	CHF_2O → CF_2O + H	CHF_2O → CHFO + F	CHF_2O → HF + FCO
B3LYP/6-31G(d,p)	−65.2	−56.5	71.3	−77.6	7.2	13.9	31.7	5.2
MP2/6-311++G(2d,2p)	−79.7	−63.8	74.6	−79.1	15.3	−0.1	20.4	−15.9
QCISD/6-311++G(2d,2p)	−68.5	−47.8	74.9	−69.4	8.9	12.6	22.5	−8.2
QCISD(T)/6-311++G(2d,2p)	−70.5	−50.5	73.3	−70.3	9.9	9.9	22.0	-10.1
QCISD(T)/6-311++G(2df,2p)	−70.3	−54.4	74.8	−73.3	10.5	8.5	24.6	−7.5
ΔZPE	1.3	−0.8	1.0	+5.4	−0.3	−5.9	−1.6	−3.0
QCISD(T)/6-311++G(2df,2p) + ΔZPE	−69.0	−55.2	75.8	−67.9	10.2	2.6	23.0	−10.5
expt.	−71.7±2	−58.7±1	71.7±2			2.6		

TABLE 7: Barrier Heights (kcal mol^{-1}) for CF_2 + OH Reaction Pathways

	CF_2OH →			CHF_2O →		
level of theory	FCO + HF	CF_2O + H	CHF_2O	CF_2O + H	CHFO + F	FCO + HF
B3LYP/6-31G(d,p)	41.3	31.6	37.8	21.3	28.2	27.2
MP2/6-311++G(2d,2p)	44.9	43.0	41.4	36.3	37.2	35.2
QCISD/6-311++G(2d,2p)	48.9	40.2	43.2	23.4	31.0	41.9
QCISD(T)/6-31++G(2d,2p)	45.7	38.4	41.7	21.1	30.6	37.2
QCISD(T)/6-311++G(2df,2p)	46.9	37.2	40.7	19.7	30.0	37.3
ΔZPE	−4.1	−5.3	−3.3	−4.8	−1.2	−2.2
QCISD(T)/6-311++G(2df,2p) + ΔZPE	42.8	31.9	37.4	14.9	28.8	35.2

p_x orbital on the oxygen into the antibonding orbital of oxygen in the in-plane p_z orbital.

B. Mechanism for the Reaction of CF_2 + OH. In the reaction of CF_2 with OH radicals, it has been suggested that the major products are CF_2O + H and CO + HF + F.[10] There are several channels which can produce CF_2O. One route involves hydrogen fission from the CF_2OH intermediate, while another involves hydrogen fission from the CHF_2O intermediate. Other possible channels for the CF_2 + OH potential energy surface are summarized in Scheme 1.

1. *Addition of CF_2 + OH.* We explored the reaction pathway for the addition of CF_2 radicals to OH radicals (reaction I in Scheme 1). A search along the CO bond coordinate did not reveal the existence of a first-order saddle point. The formation of the CO bond in CF_2OH was along a smooth surface as it proceeded to produce the CF_2OH intermediate. The formation of CF_2OH is also a downhill process, i.e., −67.9 kcal mol^{-1} at the QCISD(T)/6-311++G(2df,2p) level of theory.

TABLE 8: Heats of Formation for Reactants and Products in the CF_2+OH Reaction

species	$\Delta H_{f,0}°$ kcal mol^{-1}	reference
H	51.63 ± 0.001	*a*
F	18.47 ± 0.07	*a*
HF	−65.129 ± 0.2	*a*
CF	60.1 ± 2	*a*
OH	9.17 ± 0.29	*a*
HOF	−22.807 ± 1	*a*
FCO	−42.0 ± 4	*b*
CF_2	−43.61 ± 1.5	*a*
CF_2O	−144.8 ± 1	*c*
CHFO	−91.6 ± 1.7	*d*

[a] *JANAF Thermochemical Tables*, 3rd ed.; Chase, M. W., Jr.; Davies, C. A.; Downey, J. R.; Frurip, D. J.; McDonald, R. A.; Syrerud, A. N., Eds.; *J. Phys. Chem. Ref. Data Suppl.* **1985**, 14. [b] Bowers, M. T.; Chau, W. *J. Phys. Chem.* **1976**, *80*, 1738. [c] Montgomery, J. A., Jr.; Michels, H. H.; Francisco, J. S. *Chem. Phys. Lett.* **1994**, *220*, 391. [d] Schneider, W. F.; Wallington, T. J. *J. Phys. Chem.* **1994**, *98*, 7448.

2. *Decomposition Pathways of the CF_2OH Intermediate.* Once the CF_2OH intermediate is formed, the intermediate has a high excess of internal energy (i.e., about 67.9 kcal mol^{-1}). This energy may be sufficient to drive the CF_2OH intermediate

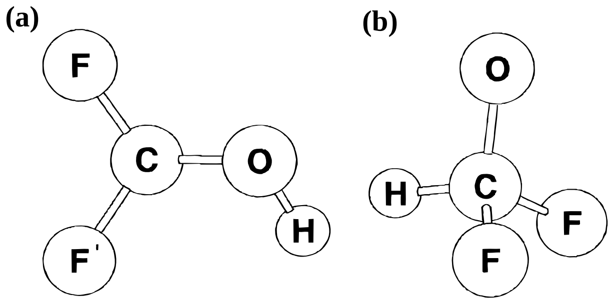

Figure 1. Intermediates in the $CF_2 + OH$ reaction. (a) Structure for the CF_2OH intermediate. (b) Structure for the CHF_2O intermediate.

SCHEME 1

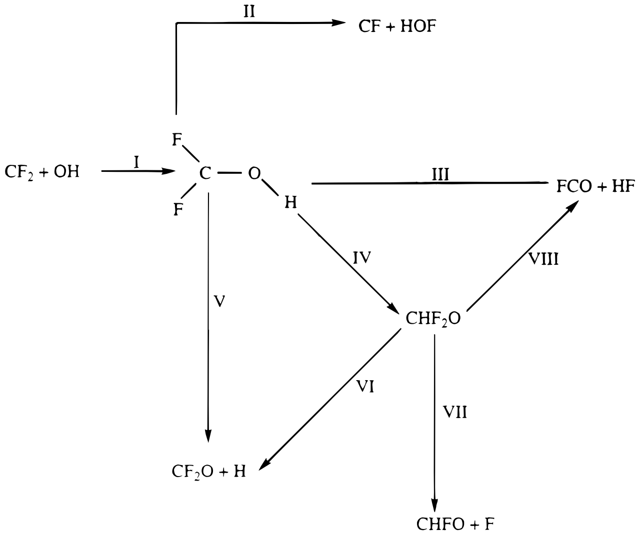

to dissociate into various products such as into CF + HOF (reaction II in Scheme 1), FCO + HF (reaction III in Scheme 1), $CF_2O + H$ (reaction V in Scheme 1), or to isomerize into CHF_2O radicals (reaction IV in Scheme 1).

Searches for a transition state along the pathway leading to the products CF + HOF were not successful in locating a first-order saddle point. However, it is unlikely that the products from the dissociation of the CF_2OH intermediate is via the CF + HOF channel since the energy requirement is estimated as 75.8 kcal mol^{-1}, in excess of the available 67.9 kcal mol^{-1} internal energy in the CF_2OH intermediate.

An examination of the pathway leading to the FCO + HF products located a transition state. This transition state, shown in Figure 2a, proceeds through a four-center intermediate. In the transition state, the CF′ bond extends to 1.730 Å and the OH bond extends to 1.207 Å; this is 28.5% longer than the CF′ bond and 25.5% longer than the OH bond in the CF_2OH intermediate. The HOC angle is 80.5°, and the F′CO angle is 91.3°. The corresponding HF bond is 36.7% longer than its final equilibrium value. These structural changes suggest that the $CF_2OH \rightarrow FCO + HF$ reaction has a relatively late transition state. The vibrational frequencies in Table 4 show that the transition state is a first-order saddle point with one imaginary frequency at 1652i. The heat of reaction for the conversion of CF_2OH radicals into FCO and HF is -1.1 kcal mol^{-1} at the QCISD(T)/6-311++G(2df,2p) level of theory. However, the barrier height is estimated to be 42.8 kcal mol^{-1}. Note that for FCO to further dissociate into F atoms and CO, another ca. 34 kcal mol^{-1} barrier must be overcome to break the CF bond in FCO. Given that 42.8 kcal mol^{-1} would have to be used to overcome the $CF_2OH \rightarrow FCO + HF$, assuming the remaining excess energy would be equally partitioned between the fragments, about 13 kcal mol^{-1} of energy should be left in the FCO fragment. This is insufficient to drive FCO across its 34 kcal mol^{-1} barrier and hence to the formation of the F + CO + HF products via this channel.

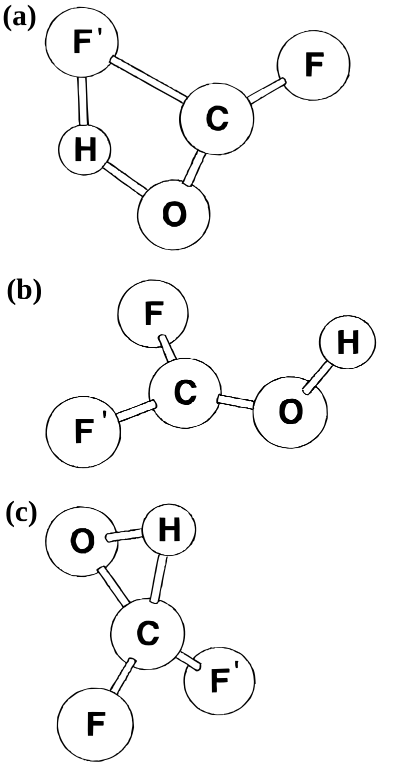

Figure 2. Structures for the transition states in the $CF_2 + OH$ reaction. (a) $CF_2OH \rightarrow FCO + HF$, (b) $CF_2OH \rightarrow CF_2O + H$, (c) $CF_2OH \rightarrow CHF_2O$.

The channel in which hydrogen-bond fission occurs from the CF_2OH radical to yield $CF_2O + H$ (reaction V in Scheme 1) could be competitive with the FCO + HF route. The transition state for this channel occurs at an OH distance of ~1.322 Å (see Figure 2b). Vibrational frequency calculations show one imagery frequency at 1371i cm^{-1} and confirms that this transition state is a first-order saddle point. The products (CF_2O + H) are 12.7 kcal mol^{-1} above the CF_2OH intermediate at the QCISD(T)/6-311++G(2df,2p) level of theory. The barrier required for this reaction to proceed is 31.9 kcal mol^{-1}. This barrier is 10.9 kcal mol^{-1} lower than the barrier for the route to proceed to the FCO + HF products.

A question raised is whether the reaction of $CF_3OH \rightarrow CHFO + F$ occurs. For the $CF_2OH \rightarrow CHFO + F$ reaction to take place, there should be a C−F bond cleavage and a hydrogen migration from O to C. Both of them cost energy. If they occur concertedly, the activation barrier must be higher than those of a stepwise process. A favorable stepwise process is $CF_2OH \rightarrow CHF_2O \rightarrow CHFO + F$. Another stepwise process is $CF_2OH \rightarrow FCOH + F \rightarrow CFHO + F$, but in this case the intermediate F−C−O−H must be very high in energy. In fact, a preliminary calculation of the energetics for this pathway shows that the energetics for $CF_2OH \rightarrow FCOH + F$ is ca. 75.8 kcal mol^{-1}. The transition states connecting this intermediate should be even higher in energy if it exists.

We ask the question whether the isomerization of CF_2OH into CHF_2O radicals (reaction IV in Scheme 1) competes with the hydrogen-bond fission channel (reaction V in Scheme 1).

A transition state for the isomerization pathway was located. The transition state is shown in Figure 2c and is a three-center state in which there is a hydrogen transfer from the oxygen atom at the OH group of CF_2OH to the carbon atom. The HO bond length is 1.235 Å, and the CH bond length is 1.260 Å. The HO bond length is elongated by 28.4% from its equilibrium position in CF_2OH. The CH bond is nearly 15.4% of the equilibrium bond in the CHF_2O radical. The HOC angle in the transition state is 57.4°. The heat of reaction for isomerization is estimated as 10.2 kcal mol^{-1} at the QCISD(T)/6-311++G(2df,2p) level of theory, but the isomerization barrier is estimated to be 37.4 kcal mol^{-1}. Note that this barrier is 5.5 kcal mol^{-1} above reaction V which yields the products CF_2O + H. The lowest energetic pathway is reaction V to yield CF_2O + H; however, we note that the isomerization channel (reaction IV) could compete with this channel. A question we now address is what the reaction pathways for CHF_2O radicals and the expected products are if this intermediate is formed.

3. *Decomposition Pathways of the CHF_2O Intermediate.* There are several dissociation channels for the CHF_2O intermediate: (1) hydrogen-bond fission (reaction VI); (2) fluorine-atom fission (reaction VII); and 1,1 elimination of HF (reaction VIII). Transition states have been located for all three reactions. In both the hydrogen-atom and the fluorine-atom fission reactions, the extruding bond comes off near 90° degrees to the COF_2 unit in the case of reaction VI and to the CHFO unit for reaction VII. This is illustrated in Figure 3a,b. The CF′ bond in the transition state (1.785 Å) is quite similar to that in the extruding CF bond in CF_3O going to CF_2O + F (1.762 Å). As expected, the CH and CF bonds in the transition state are quite similar to the reactant CHFO; however, the CO bond is longer, i.e., 1.210 Å, than that in CHFO. This is because there is a hybridization which occurs for the CO bond (which is sp^3 hybridized in the CHF_2O radical) as it goes on to form CHFO in which the CO bond is sp^2 hybridized. Similar structural trends are seen in the transition state for reaction V for the hydrogen atom fission process.

With the CHF_2O radical, an interesting question to ask is which process is more facile: hydrogen-atom vs fluorine-atom bond fission. Thermodynamically, the hydrogen-atom bond fission process is more favored, being 2.5 kcal mol^{-1} versus 23.0 kcal mol^{-1} for the fluorine-atom bond fission process. The kinetics, as governed in part by the barrier height, determine the relative importance and rate ordering for these two processes. For hydrogen-atom bond fission, the barrier height is 14.9 kcal mol^{-1}, while for fluorine-atom bond fission it is 28.8 kcal mol^{-1}. Consequently, the hydrogen-atom bond fission should be thermodynamically and kinetically favored over the fluorine-atom bond fission process. However, the 1,1 HF-elimination pathway on thermodynamic grounds is competitive with the hydrogen-atom bond fission process at the QCISD(T)/6-311++G-(2df,2p)//UMP2/6-311++G(2d,2p) level of theory. We located a transition state for the 1,1 HF-elimination pathway (Figure 3c). The transition is a tight-transition state in which the hydrogen migrates toward the fluorine. In the process, the CH and CF bonds elongate to 17.8% and 20.8%, respectively, to the bond length in the CHF_2O radical. The forming HF′ bond is 49.6% of the HF bond in HF. The barrier height for the 1,1 HF-elimination process is quite high, being 35.2 kcal mol^{-1}. Although thermodynamically, the 1,1 HF-elimination process is favored over the hydrogen-atom bond fission process, on kinetic grounds the hydrogen atom process is the more favored. Its barrier is 20.3 kcal mol^{-1} less than that for the 1,1 HF-elimination pathway.

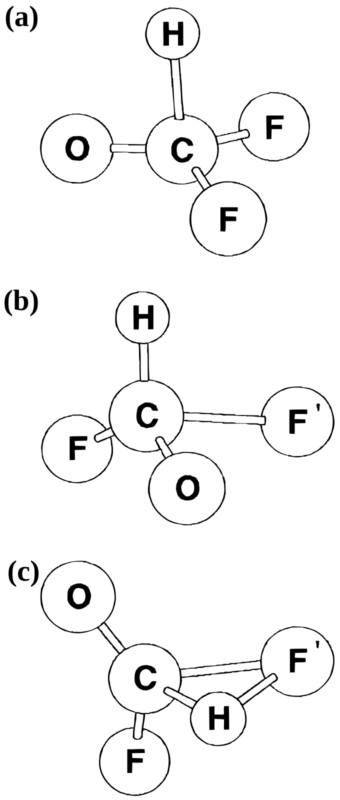

Figure 3. Structures for the transition state in the CF_2 + OH reaction. (a) $CHF_2O \rightarrow CF_2O + H$, (b) $CHF_2O \rightarrow CHFO + F$, (c) $CHF_2O \rightarrow FCO + HF$.

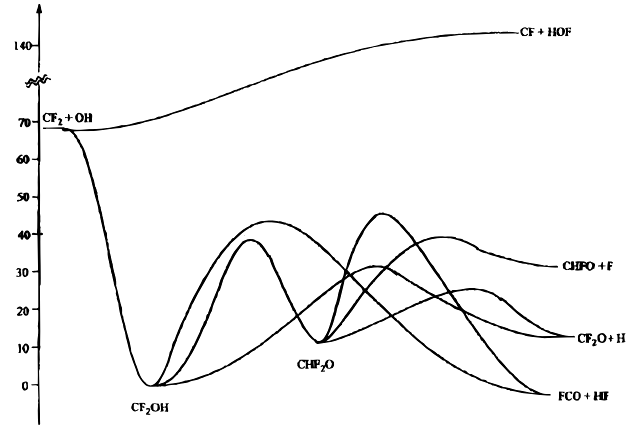

Figure 4. Summary of the CF_2 + OH potential energy surface calculated at the QCISD(T)/6-311++G(2df,2p)//UMP2/6-311++G-(2d,2p) level of theory (values are in kcal mol^{-1}).

C. Summary of the CF_2 + OH Reaction Potential Energy Surface. A summary of the potential energy surface for CF_2 + OH is shown in Figure 4. The present calculations suggest the following about the mechanism for the CF_2 + OH reaction: (1) the first step of the reaction is the addition of the CF_2 radical to OH which produces the CF_2OH intermediate, and (2) the CF_2OH intermediate can dissociate to produce CF_2O and H atoms via

$$CF_2 + OH \rightarrow CF_2OH^* \rightarrow CF_2O + H \qquad (2)$$

We found that there is a competitive pathway involving (1) isomerization of the CF_2OH radical, followed by the dissociation of the newly formed CHF_2O radicals into CF_2O and H atoms, via

$$CF_2 + OH \rightarrow CF_2OH^* \rightarrow CHF_2O^* \rightarrow CF_2O + H \quad (3)$$

This pathway is 5.5 kcal mol^{-1} below the route leading to CF_2O + H (reaction 2). Since both processes will be driven by the available internal energy in the CF_2OH intermediate formed from the CF_2 + OH addition reaction, any quenching of CF_2OH could significantly impact the branching ratio of the second channel (reaction 3). We also note that both pathways contribute to the formation of the CF_2O and H atoms. Thus, from our survey of the mechanism of the CF_2 + OH reaction, we find that the major products of the reaction are H and CF_2O. This also suggests that experimentally, if one monitors only the products, it would be difficult to determine the mechanistic routes, since there are two channels leading to the same final products. We do find a channel whereby the products HF + CO + F are produced as suggested by Biordi et al.[10] It is quite possible that in flames, this channel could be competitive, but it may be a minor channel. The suggestion of CF_2O as a major product is consistent with experimental studies that have observed it in flames seeded with fluorocarbons.[4,6,8]

IV. Conclusion

The potential energy surface of the CF_2 + OH reaction has been examined using density functional and Møller−Plesset perturbation methods. There are two intermediates that may play a role in this reaction: CF_2OH and CHF_2O. The transition states involved in the reaction system have been located and optimized. The complete reaction mechanism has been suggested for the first time based on *ab initio* calculations. The CF_2 + OH reaction can proceed through either the CF_2OH or the CHF_2O intermediates, both decomposing to form CF_2O + H. Consequently, the only expected final products of the reaction are the CF_2O and H atoms. The heat of reaction for the net process is estimated as −55.2 kcal mol^{-1} at the QCISD(T)/6-311++G(2df,2p)//UMP2/6-311++G(2d,2p) level of theory. There is no net activation barrier that has to be surmounted for this process, and the reaction should be driven by the internal exothermic energy in the CF_2OH intermediate formed from the addition of CF_2 radicals with OH.

References and Notes

(1) Singh, H. B. *Composition, Chemistry and Climate of the Atmosphere*, H. B. Singh, Ed.; Van Nostrand Reinhold: New York, 1995; pp 216−250.

(2) Prather, M. J.; Watson, R. T. *Nature* **1990**, *344*, 729.

(3) McCulloch, A. *Atmos. Environ.* **1992**, *26A*, 1325.

(4) Linteris, G. T.; Burgess, D. R.; Babushok, V.; Zachariah, M.; Tsang, W.; Westmoreland, P. *Combust. Flame* **1998**, *113*, 164.

(5) Sanogo, O.; Delfau, J.; Akrich, R.; Vovello, C. Twenty-Fifth International Symposium on Combusion, Proceedings; The Combustible Institute, Pittsburgh, 1994; p 1489.

(6) Battin-Leclerc, F.; Wolravens, B.; Come, G. M.; Baronnet, F.; Sanogo, O.; Delfau, J.; Vavelle, C. ACS Symposium Series 611, Halon Replacement, American Chemical Society: Washington, D.C., 1995; p 289.

(7) Burgess, D. R.; Zachariah, M. R.; Tsang, W.; Westmoreland, P. R. *Prog. Energy Combust. Sci.* **1996**, *21*, 453.

(8) McNesby, K. L.; Daniel, R. G.; Widder, J. M.; Miziolek, A. W. *App. Spectrosc.* **1996**, *50*, 126.

(9) Su, Y.; Gu, Y.-W.; Reck, G. P.; Rothe, E. W.; Francisco, J. S. *Combust. Flame* **1998**, *113*, 236.

(10) Biordi, J. C.; Lazzara, C. P.; Papp, J. F. *J. Phys. Chem.* **1976**, *80*, 1042.

(11) Frisch, M. J.; Trucks, G. W.; Schlegel, H. B.; Gill, P. M. W.; Johnson, B. G.; Robb, M. A.; Cheeseman, J. R.; Keith, T. A.; Petersson, G. A.; Montgomery, J. A.; Raghavachari, K.; Al-Laham, M. A.; Zakrzewski, V. G.; Ortiz, J. V.; Foresman, J. B.; Cioslowski, J.; Stefanov, B. B.; Nanayakkara, A.; Challacombe, M.; Peng, C. Y.; Ayala, P. Y.; Chen, W.; Wong, M. W.; Andres, J. L.; Replogle, E. S.; Gomperts, R.; Martin, R. L.; Fox, D. J.; Binkley, J. S.; Defrees, D. J.; Baker, J.; Stewart, J. J. P.; Head-Gordon, M.; Gonzalez, C.; Pople, J. A. *GAUSSIAN 94*; Gaussian, Inc.: Pittsburgh, 1995.

(12) Schlegel, H. B. *J. Chem. Phys.* **1986**, *84*, 4530.

(13) Becke, A. D. *J. Chem. Phys.* **1993**, *98*, 1372.

(14) Lee, C.; Yang, W.; Parr, R. G. *Phys. Rev. B* **1988**, *41*, 785.

(15) Møller, C.; Plesset, M. S. *Phys. Rev.* **1934**, *46*, 618.

(16) Pople, J. A.; Binkley, J. S.; Seeger, R. *Int. J. Quantum. Chem. Symp.* **1976**, *10*, 1.

(17) Pople, J. A.; Head-Gordon, M.; Raghavachari, K. *J. Chem. Phys.* **1987**, *87*, 5968.

(18) Knowles, P. J.; Werner, H. J. *Chem. Phys. Lett.* **1985**, *115*, 259.

(19) Werner, H. J.; Knowles, P. J. *J. Chem. Phys.* **1985**, *82*, 5053.

(20) Werner, H. J.; Knowles, P. J. *J. Chem. Phys.* **1988**, *89*, 5803.

(21) MOLPRO is a package of *ab initio* molecular orbital theory programs written by H. J. Werner and P. J. Knowles with contributions from J. Almlöf, R. D. Amos, M. J. O. Deegan, S. T. Elbert, C. Hampel, W. Meyer, K. A. Peterson, R. M. Pitzer, A. J. Stone, P. R. Taylor, and R. Lindh.

(22) Francisco, J. S.; Zhao, Y. *J. Chem. Phys.* **1990**, *93*, 276.

(23) Francisco, J. S.; Li, Z.; Williams, I. H. *Chem. Phys. Lett.* **1991**, *186*, 343.

(24) Li, Z.; Francisco, J. S. *Chem. Phys. Lett.* **1991**, *186*, 336.

(25) Saathoff, H.; Zellner, R. *Chem. Phys. Lett.* **1993**, *206*, 349.